

Actinide Metals with Multiple Bonds to Carbon: Synthesis, Characterization, and Reactivity of U(IV) and Th(IV) Bis(iminophosphorano)methandiide Pincer Carbene Complexes

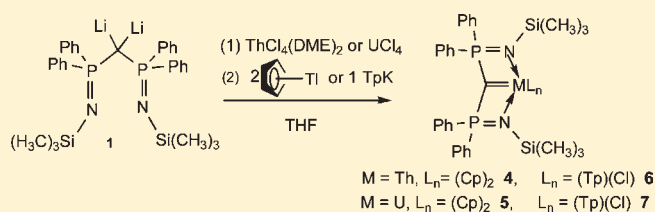
Guibin Ma, Michael J. Ferguson,[†] Robert McDonald,[†] and Ronald G. Cavell*

Department of Chemistry and [†]X-ray Structure Determination Laboratory, University of Alberta, Edmonton, Alberta, Canada T6G 2G2

S Supporting Information

ABSTRACT: Treatment of ThCl₄(DME)₂ or UCl₄ with 1 equiv of dilithiumbis(iminophosphorano) methandiide, [Li₂C(Ph₂P=NSiMe₃)₂] (1), afforded the chloro actinide carbene complexes [Cl₂M(C(Ph₂P=NSiMe₃)₂)] (2 (M = Th) and 3 (M = U)) in situ. Stable PCP metal–carbene complexes [Cp₂Th(C(Ph₂P=NSiMe₃)₂)] (4), [Cp₂U(C(Ph₂P=NSiMe₃)₂)] (5), [TpTh(C(Ph₂P=NSiMe₃)₂)Cl] (6), and [TpU(C(Ph₂P=NSiMe₃)₂)Cl] (7) were generated

from 2 or 3 by further reaction with 2 equiv of thallium(I) cyclopentadienide (CpTl) in THF to yield 4 or 5 or with 1 equiv of potassium hydrotris(pyrazol-1-yl) borate (TpK) also in THF to give 6 or 7, respectively. The derivative complexes were isolated, and their crystal structures were determined by X-ray diffraction. All of these U (or Th)–carbene complexes (4–7) possess a very short M (Th or U)=C double bond with evidence for multiple bond character. Gaussian 03 DFT calculations indicate that the M=C double bond is constructed by interaction of the 5f and 6d orbitals of the actinide metal with carbene 2p orbitals of both π and σ character. Complex 3 reacted with acetonitrile or benzonitrile to cyclo-add C≡N to the U=C double bond, thereby forming a new C–C bond in a new chelated quadridentate ligand in the bridged dimetallic complexes (9 and 10). A single carbon–U bond is retained. The newly coordinated uranium complex dimerizes with one equivalent of unconverted 3 using two chlorides and the newly formed imine derived from the nitrile as three connecting bridges. In addition, a new crystal structure of [CpUCl₃(THF)₂] (8) was determined by X-ray diffraction.



INTRODUCTION

Binding of two-electron carbene donors to metal ions to form complexes with carbon–metal bonds plays a central role in catalytic organometallic chemistry,¹ and for many main-group and d-block elements, this chemistry has reached an advanced stage of development.² However, the development of actinide (5f) carbene complexes has not been extensively pursued. In pioneering work, Gilje et al. prepared uranium phosphoylide carbene compounds such as (η⁵-C₅H₅)₃U=CHP(CH₃)₂(C₆H₅) and several relatives thereof which were the first actinide carbenes to be structurally characterized.^{3f,g} No thorium carbene complexes have been reported in the literature. Recently, adducts of neutral N-heterocyclic carbene (NHCs) to the UO₂²⁺ and UI²⁺ ions and to Cp*₂UI have been prepared, yielding complexes such as UO₂-Cl₂L₂^{4a} (L = 1,3-dimesitylimidazole-2-ylidene (IMes) or 1,3-dimesityl-4,5-dichloroimidazole-2-ylidene (IMesCl₂)), UIL₃^{4b} (L = OCMe₂CH₂[1-C(NCHCHN)Pr]), U(C₅Me₅)₂I(C₃Me₄N₂)^{4c} and U(C₅H₄Bu^t)₃(C₃Me₄N₂)^{4c}. In contrast to these relatively sparse examples, uranium complexes with organoimido or hydrocarbyl ligands are fairly numerous.³ The N-heterocyclic carbene (NHC) ligands are well-known to be strong σ-donor ligands, so formation of these NHC–metal complexes are considered to be simple Lewis base adducts possessing a single C–M bond with no significant multiple carbene–metal bond character,

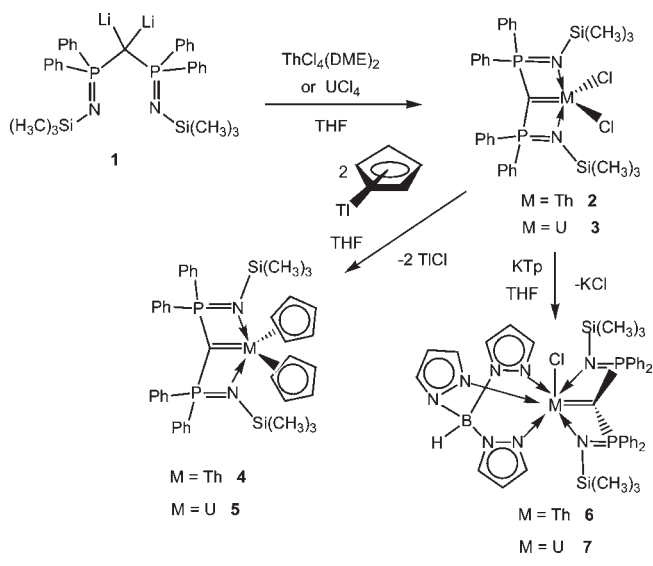
and it is thought that the intrinsic electronic properties of these metals does not allow stabilization of the carbene center.⁵ A few species of the form [M]=CH₂ (M = Ce, Nd, Th, U) have been detected by IR spectroscopy in reactions of excited metal atoms with methane or methyl halides in solid argon.⁶ Carbenoid [U]=CR₂ nucleophilic species were suggested in McMurry type reactions of sterically hindered ketones in the UCl₄/Li(Hg) system.⁷ We have undertaken an exploration of our bis(iminophosphorano)methandiide system with lanthanides and actinides with a view of establishing whether involvement of 4f and 5f orbitals and development of M–C multiple bonds could be established with these elements. Very recently, several uranium nucleophilic carbene complexes with the related SCS (SCS = (Ph₂P=S)₂C²⁻) ligand and alternatively substituted NPCPN²⁻ methandiide pincer carbene complexes were obtained and structurally characterized.⁸

We developed the bis(iminophosphorano)methandiide pincer carbene ligand system by means of double deprotonation of a neutral bis(iminophosphorane) through dilithiation of the ligand followed by metathetical lithium halide elimination or by reacting the ligand with appropriate metal precursors to eliminate alkyls

Received: December 20, 2010

Published: June 13, 2011

Scheme 1. Synthesis of Complexes



or other protonated species, and an interesting body of chemistry for transition, main group, and noble metals has emerged.⁹ Previously, the only reported lanthanide metal complex of this carbene ligand was the Sm(III) carbene double bond complex $[\text{Sm}=\text{C}(\text{Ph}_2\text{P}=\text{NSiMe}_3)_2(\text{NCy})]^{9g}$; however, others have recently prepared additional examples of the lanthanide complexes with the Mes-substituted bis(iminophosphorano)methandiide analog.^{9r} We have now extended our studies of metal complexes of this system to the 5f actinide group, specifically Th and U, thereby providing new extensions to the examples of doubly bound carbene–actinide metal complexes of the dianionic methandiide ligand system derived from $[\text{Li}_2\text{C}(\text{Ph}_2\text{P}=\text{NSiMe}_3)_2]_2$ (**1**).¹⁰

RESULTS AND DISCUSSION

Synthesis of the Complexes. A red, air-sensitive, presumably monomeric, crystalline solid complex of Th(IV), $[\text{Cp}_2\text{Th}\{\text{C}(\text{Ph}_2\text{P}=\text{NSiMe}_3)_2\}]$ (**4**), was obtained when 1 equiv of dimeric $[\text{Li}_2\text{C}(\text{Ph}_2\text{P}=\text{NSiMe}_3)_2]_2$ (**1**)¹⁰ was added to a THF solution of 2 equiv of $\text{ThCl}_4(\text{DME})_2$ under an argon atmosphere. Ultimately, because **2** could not be crystallized, we then added, directly, two equivalents of solid thallium(I) cyclopentadienide, TICp , per equivalent of **2** to give **4**. Successful Cp substitution was indicated by the generation of white, insoluble, solid TICl . Complex **4** crystallized nicely and was fully structurally and analytically characterized. As an alternative to Cp substitution, we also converted the dichloride complex, **2**, to the pyrazolyl borate complex, $[\{\text{HB}(\text{pyrazolyl})_3\}\text{Th}\{\text{C}(\text{Ph}_2\text{P}=\text{NSiMe}_3)_2\}\text{Cl}]$ (**6**), with 1 equiv of TpK (Scheme 1), which provided good crystals. Similarly, two U(IV) complexes were prepared as green air-sensitive crystalline solids. The first, $[\text{Cp}_2\text{U}\{\text{C}(\text{Ph}_2\text{P}=\text{NSiMe}_3)_2\}]$ (**5**), was prepared from UCl_4 and **1** followed by treatment with TICp in an exactly parallel fashion to the preparation of **4** and the second, $[\{\text{HB}(\text{pyrazolyl})_3\}\text{U}\{\text{C}(\text{Ph}_2\text{P}=\text{NSiMe}_3)_2\}\text{Cl}]$ (**7**), by treatment of intermediate **3** with 1 equiv of TpK . These derivatized complexes also crystallized nicely and were fully analytically and structurally characterized. Although we did not succeed in crystallizing the chloro compounds **2** and **3** from the reaction solutions, the derivatizations to the fully characterized species **4–7** clearly established the

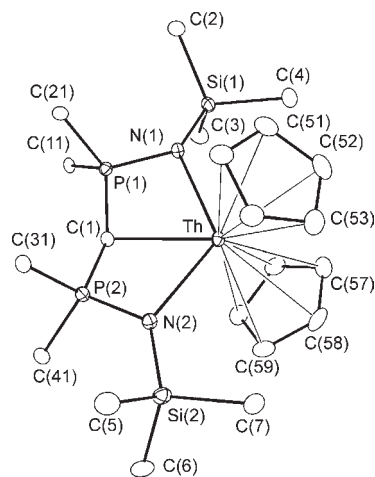


Figure 1. Perspective view of the $[(\eta^5\text{-C}_5\text{H}_5)_2\text{Th}\{\kappa^3\text{-C}(\text{Ph}_2\text{P}=\text{NSiMe}_3)_2\}]$ (**4**) molecule showing the atom labeling scheme. Only the ipso carbons of the phenyl rings are shown. Non-hydrogen atoms are represented by Gaussian ellipsoids at the 20% probability level. Hydrogen atoms are not shown. The structure of the analogous, isostructural uranium complex (**5**) is given in the Supporting Information.

identities of **2** and **3**. The result of the reactions of **3** with nitriles described below is also supportive of the identity and formulation of **3**. Interestingly, initial attempts to prepare the analogous $\text{SPPH}_2\text{CPPH}_2\text{S}$ dianionic complex (SCS^{2-}) directly from UCl_4 and $\text{Li}_2(\text{SCS})$ by others was not successful due to solubility problems and interfering ligand and solvent interactions, and accordingly alternate routes were necessary.^{8a} In this case, successful syntheses of a series of uranium(IV) complexes were achieved using a $\text{U}(\text{BH}_4)_4$ precursor. Three complexes (two containing three SCS ligands and one pincer monomer complex) were obtained.^{8a} Later, this group successfully prepared pincer SCS complexes (including a bis(carbene)) with both Cl or Cp substituents directly from UCl_4 .^{8b} Others have used the methylene backbone NMe's analog of **1** to obtain a uranium(IV) complex containing two NCN pincer substituents (as a bis(carbene)) by a substitution–disproportionation reaction from UI_3 .^{8c}

The NMR spectra of the diamagnetic complexes **4** and **6** were normal with all chemical shifts in the predicted regions. Multiplicities expected from the presence of two ^{31}P nuclei were observed. Complexes **5** and **7** are paramagnetic, so NMR resonances are broad and display paramagnetic shifts; the ^{31}P NMR spectra of **5** and **7** each consisted of one broad singlet at 361.62 and -381.7 ppm, respectively. The signal for **5** is downfield shifted by 347.2 ppm with respect to the ^{31}P shift value for compound **1** (14.4 ppm), and that for **7** is upfield shifted by 396.1 ppm. The proton NMR for complex **5**, showed downfield shifts for phenyl protons and upfield shifts for the $-\text{Si}(\text{CH}_3)_3$ and Cp protons. No signal was observed in the $^{13}\text{C}\{^1\text{H}\}$ NMR spectrum for the quaternary backbone carbon for these complexes, fairly typical behavior for these carbene centers.^{9j}

Crystal Structures and Bond Lengths in the Complexes. The molecular structures of $[(\eta^5\text{-C}_5\text{H}_5)_2\text{Th}\{\kappa^3\text{-C}(\text{Ph}_2\text{P}=\text{NSiMe}_3)_2\}]$ (**4**), $[(\eta^5\text{-C}_5\text{H}_5)_2\text{U}\{\kappa^3\text{-C}(\text{Ph}_2\text{P}=\text{NSiMe}_3)_2\}]$ (**5**), $[\{\text{HB}(\text{pyrazolyl})_3\}\text{Th}\{\kappa^3\text{-C}(\text{Ph}_2\text{P}=\text{NSiMe}_3)_2\}\text{Cl}]$ (**6**), and $[\{\text{HB}(\text{pyrazolyl})_3\}\text{U}\{\kappa^3\text{-C}(\text{Ph}_2\text{P}=\text{NSiMe}_3)_2\}\text{Cl}]$ (**7**) were confirmed by X-ray crystallography. Perspective views of thorium complexes (**4** and **6**) are shown in Figures 1 and 2. The isostructural uranium complexes (**5** and **7**) are given in the Supporting Information.

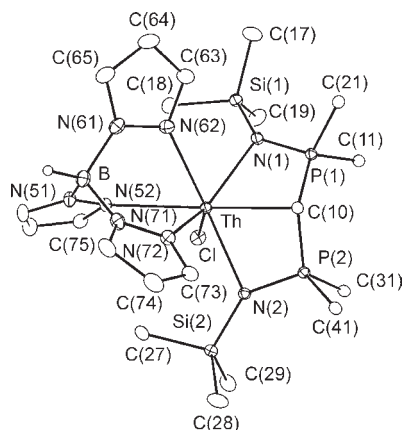


Figure 2. Perspective view of the $[\text{HB}(\text{pyrazolyl})_3]\text{Th}\{\text{C}(\text{Ph}_2\text{P}=\text{N}-\text{SiMe}_3)_2\text{Cl}\}$ (**6**) molecule showing the atom labeling scheme. Only the ipso carbons of the phenyl rings are shown. Non-hydrogen atoms are represented by Gaussian ellipsoids at the 20% probability level. The hydrogen atom of the B–H group is shown with an arbitrarily small thermal parameter; the remaining hydrogen atoms are not shown. The structure of the analogous, isostructural uranium complex (**7**) is given in the Supporting Information.

The selected bond lengths and bond angles are shown in Tables 1 and 2. The core structures of **4**–**7** are similar, consisting of two nearly planar, fused, four-membered rings with a common M–C(1) (M = Th, U) shared edge. The two planes in **4** and **5** have small dihedral angles ($7.65(14)^\circ$ for **4** and $7.62(8)^\circ$ for **5**), but the planes in structures **6** and **7**, defined by the two four-membered rings (plane 1: M, N(1), P(1), and C(10) and plane 2: M, N(2), P(2), and C(10)), have somewhat bigger dihedral angles ($32.76(9)^\circ$ for **6** and $34.24(6)^\circ$ for **7**). Foldings in this methandiide system have previously been found to range from about 30° to 0° ,^{9a,b,f–i,l} and it seems that the bonding is flexible with regard to this axis. The extent of bending is probably determined by intramolecular interactions. Intramolecular chelation of the two trimethylsilylimine units in the ligand completes the pincer carbene structure. The two η^5 -Cp rings complete the coordination around the thorium(IV) and uranium(IV) in **4** and **5**. The two Cp planes are disposed symmetrically above and below this axial (M=C) bis(chelate) pair of planes of fused four-membered rings with dihedral angles of $59.3(2)^\circ$ in **4** and $59.32(10)^\circ$ in **5**, respectively. In **6** and **7**, which are forced to functional 7 coordination by the requirements of the tridentate (three N atoms) Tp ligand and the bound Cl substituent, the Tp is sitting on the opposite side of the chloride with respect to the axial (folded) plane along the M=C axis. One of the coordinated N atoms (N(52)) is located opposite the carbene C(10) with a N(52)–M–C(10) bond angle of $166.18(11)^\circ$ for **6** and $168.28(8)^\circ$ for **7**. The uranium to carbon bond distances U–C(1) = $2.351(2)$ Å (**5**) and U–C(10) = $2.376(3)$ Å (**7**) are both considerably shorter (15%) than the average U–carbene (NHC) distances⁴ {average 2.694 Å, a range of $2.609(4)$ – $2.799(3)$ Å}; however, these lengths are slightly longer (3%) than the shortest known multiple U–C bond distance in the U–phosphonide, $2.29(3)$ Å,^{36g} and indeed they are compatible with the three recently studied uranium SCS pincer carbene complexes containing a U=C double bond (U–C = $2.327(3)$, $2.444(4)$, and $2.484(3)$ Å, respectively).^{8a} All of these distances are shorter than those found for U–C single bonds. Typical recent examples of U–C single bonds are the pincer-like complex (which bears some resemblance to the present system) tris(1,2-dimethoxyethane)-lithium- μ^2 -chloro-(μ^2 -4-oxybutyl)-1,2-dimethoxyethane)-(2,6-bis(N-(2,6-diisopropylanilino)ethen-1-

Table 1. Selected Bond Lengths (Å) and Angles (deg) for Complexes **4** and **5**

complex 4			
bond lengths (Å)			
Th–C(1)	2.436(4)	Th–C(56)	2.814(5)
Th–N(1)	2.508(3)	Th–C(57)	2.828(5)
Th–N(2)	2.501(3)	Th–C(58)	2.830(5)
Th–C(50)	2.813(5)	Th–C(59)	2.816(5)
Th–C(51)	2.849(5)	Th–C(1)	1.654(4)
Th–C(52)	2.868(5)	P(1)–C(1)	1.635(3)
Th–C(53)	2.846(5)	P(1)–N(1)	1.664(4)
Th–C(54)	2.813(5)	P(2)–C(1)	1.631(4)
Th–C(55)	2.800(5)	P(2)–N(2)	
angles (deg)			
N(1)–Th–N(2)	125.09(11)	N(2)–P(2)–C(1)	104.06(19)
N(1)–Th–C(1)	62.93(12)	P(1)–C(1)–P(2)	150.5(3)
N(2)–Th–C(1)	63.46(12)		
complex 5			
bond lengths (Å)			
U–C(1)	2.351(2)	U–C(56)	2.756(2)
U–N(1)	2.4896(18)	U–C(57)	2.771(3)
U–N(2)	2.4775(18)	U–C(58)	2.770(3)
U–C(50)	2.747(2)	U–C(59)	2.762(3)
U–C(51)	2.781(2)	U–C(1)	1.667(2)
U–C(52)	2.807(3)	P(1)–N(1)	1.6288(18)
U–C(53)	2.789(2)	P(2)–C(1)	1.667(2)
U–C(54)	2.757(2)	P(2)–N(2)	1.6253(19)
U–C(55)	2.744(2)		
angles (deg)			
N(1)–U–N(2)	127.14(6)	N(1)–P(1)–C(1)	102.59(10)
N(1)–U–C(1)	64.13(7)	P(1)–C(1)–P(2)	149.83(14)

yl)benzene)-lithium–uranium with a U–C(phenyl) single bond length of 2.476 Å.^{3j} Our U–C(methine) bond in **9** (see below) is $2.660(7)$ Å. A dimethyl-tetramethyl EDTA U(IV) complex with a six coordinate structure has U–C(methyl) bond lengths of 2.47 – 2.48 Å.^{3k} A large number of Cp and Cp* uranium(IV) examples have been reported which show U–C single bond lengths ranging around from 2.33 to 2.43 Å depending on the electronegativity of the substituent (see, for example, ref 3l and references therein). These Cp, Cp*, and related complexes are however more open than our pincers, and this may allow for shorter bonds. No Th–carbene bond data are available for comparison; however, the Th–C distances in **4** { $2.436(4)$ Å} and in **6** { $2.469(3)$ Å} are also obviously shorter (9%) than the Th–C bond distances found for previously reported hydrocarbyl thorium complexes { $2.641(5)$ Å^{11a} and $2.617(5)$ – $2.892(5)$ Å}.^{11b} These bond lengths suggest multiple bond character between the metals (U or Th) and the central ligand carbon atom for complexes **4**–**7**.

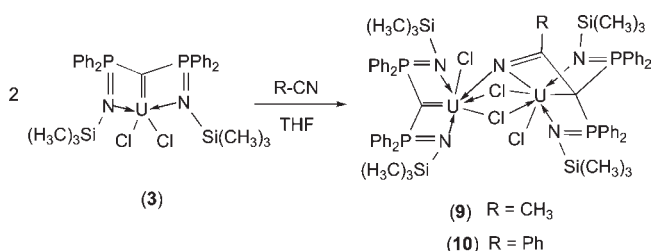
The bond distances (P–C and P–N) within the ligand framework in these complexes are also considerably altered in comparison with the related values in the free bis(iminophosphorano)methane ligand¹² and the dilithium dianionic methanide salt **1**.¹⁰ The P=N bond distances are elongated, and the endocyclic P–C bond

Table 2. Selected Bond Lengths (Å) and Angles (deg) for Complexes 6 and 7

complex 6			
bond lengths (Å)			
Th–C(10)	2.469(3)		
Th–N(1)	2.430(3)	Th–Cl	2.7264(10)
Th–N(2)	2.457(3)	P(1)–C(10)	1.683(4)
Th–N(52)	2.654(3)	P(1)–N(1)	1.633(3)
Th–N(62)	2.650(3)	P(2)–C(10)	1.668(4)
Th–N(72)	2.621(3)	P(2)–N(2)	1.640(3)
angles (deg)			
Cl–Th–N(1)	88.78(8)	Cl–Th–C(10)	112.53(8)
Cl–Th–N(2)	83.79(8)	P(1)–C(10)–P(2)	139.1(2)
Cl–Th–N(52)	80.94(8)	N(1)–Th–N(2)	120.32(10)
Cl–Th–N(62)	134.50(8)	N(1)–Th–N(52)	120.80(10)
Cl–Th–N(72)	137.26(8)	N(1)–Th–N(62)	77.85(11)
N(1)–P(1)–C(10)	104.25(16)	N(1)–Th–N(72)	133.87(11)
complex 7			
bond lengths (Å)			
U–C(10)	2.376(3)		
U–N(1)	2.389(2)	U–Cl	2.6840(7)
U–N(2)	2.405(2)	P(1)–C(10)	1.687(3)
U–N(52)	2.599(2)	P(1)–N(1)	1.628(2)
U–N(62)	2.609(2)	P(2)–C(10)	1.681(3)
U–N(72)	2.574(2)	P(2)–N(2)	1.633(2)
angles (deg)			
Cl–U–N(1)	86.88(6)	Cl–U–C(10)	111.54(7)
Cl–U–N(2)	83.34(6)	P(1)–C(10)–P(2)	138.49(17)
Cl–U–N(52)	79.89(6)	N(1)–U–N(2)	122.58(8)
Cl–U–N(62)	133.58(6)	N(1)–U–N(52)	118.90(8)
Cl–U–N(72)	137.69(6)	N(1)–U–N(62)	76.92(8)
N(1)–P(1)–C(10)	102.94(11)	N(1)–U–N(72)	135.28(8)

distances are significantly shorter. However, the exocyclic P–C distances are unaffected. The P–C–P bond angles $150.55(11)^\circ$ (4), $149.84(14)^\circ$ (5), $139.1(2)^\circ$ (6), and $138.49(17)^\circ$ (7) are considerably widened compared to the corresponding values in $\text{CH}_3\text{CH}\{\text{Ph}_2\text{P}=\text{N}(p\text{-tolyl})\}_2$ ($112.39(19)^\circ$)^{12a} and in $\text{H}_2\text{C}\{\text{Cy}_2\text{P}=\text{NSiMe}_3\}_2$ ($117.41(12)^\circ$)^{12b} and are also remarkably widened compared to $[\text{Li}_2\text{C}(\text{Ph}_2\text{P}=\text{NSiMe}_3)_2]$ ($132.6(3)^\circ$)¹⁰ and $[\text{Sm}\{\text{C}(\text{Ph}_2\text{P}=\text{NSiMe}_3)_2\}(\text{NCy}_2)]$ ($138.0(3)^\circ$)^{9b}. These factors suggest that there is a delocalization of π electron density within each of the four-membered metallocyclic rings, via conjugation of M=C (M = Th, U) and P=N bonds. That the two four-membered metallocyclic rings are nearly coplanar is an indication of strong carbene to actinide metal and π electron delocalization interactions.

During the course of precursor preparation, we isolated compound 8 ($\text{CpUCl}_3(\text{THF})_2$) as deep green crystals from the reaction mixture of UCl_4 with 1 equiv of CpTiI in THF. Although previously synthesized,^{13a,b} no structure was reported. We have structurally characterized this interesting precursor, and the results are given in the Supporting Information. The structure is quite similar to that of $\text{MeCpUCl}_3(\text{THF})_2$, which was reported some time later than the original syntheses of the original relatives.^{13c}

Scheme 2. Reactivity of the U=C Double Bond with Nitriles, R–C≡N

Reactivity of the Uranium Complexes. Many years ago, Gilje et al. studied the reactivity of the phospholide uranium–carbon multiple bond in the system $\text{Cp}_3\text{U}=\text{CHPR}_3$ toward CO ,^{14a} isonitrile, or nitrile,^{14b} which resulted in insertion reactions to the U=C double bond and the formation of new ligands in the uranium coordination sphere. The new ligands replaced the U=C bond with a bond between C and also O of the reactant. Recently, Mézailles et al. studied the reactivity of their U=C (SCS) carbene complexes toward molecules containing a carbonyl function such as ketones and aldehydes.^{8a} In these cases, the C=O center added to the carbene center, and a tetrasubstituted olefin was eliminated to break the M=C bond and the pincer structure. Presumably, a metal oxo complex was also formed, as the eliminated organic products contained no oxygen.

The chemical reactivity of the U=C multiple bond in the intermediate 3 was explored with a solution study of reactivity with nitriles (acetonitrile and benzonitrile). In these cases, the C≡N triple bond suffered a 1,2 cycloaddition to the carbon–metal bond to form a new C–C bond and build a new tetradentate ligand (with three imine centers which coordinate to the U while maintaining a single U–C bond), as shown in Scheme 2. Thus, reactions of either acetonitrile or benzonitrile with 1 equiv of 3 in situ (THF) at room temperature (about 25 °C) formed complexes 9 and 10, respectively, in almost quantitative yields, and only 1/2 of the quantity of 3 was transformed. The newly formed (carbon) imine center joins with two of the chlorides to form a bridged complex with the remaining half of the starting complex, 3. The reaction pathways demonstrated by the present uranium methandiide complex provide a contrast with the behavior of U=C centers reported by previous workers.^{8a,14}

The crystal structure of 9 was solved by X-ray diffraction. The molecular structure is shown in Figure 3a, and the selected bond distances and angles are listed in Table 3. The structure has two separated (and different) pincer carbon complexed uranium metal centers linked to each other by two chlorides and one nitrogen atom (a carbon imine center derived from the insertion of the nitrile into one of the U=C bonds). As a result, one pincer unit contains a uranium methandiide (U=C) center; the other pincer U center is formed with a uranium–methine carbon center. Both PCP pincer units are bound by the aforementioned bridges such that each metal achieves seven coordination. The U=C(methandiide) bond is shorter (distance U(1)–C(1) = 2.337(7) Å) than similar bonds in 5 (bond distance U–C(1) = 2.351(2) Å) and 7 (bond distance U–C(2) = 2.376(3) Å). The other has a U–C single bond (distance U(2)–C(2) = 2.660(7) Å). The difference in bond lengths (the U–C (2) distance is 13% longer than the U=C(1) distance) is consistent with a reduction in bond order in one case from a formal metal–carbon double bond

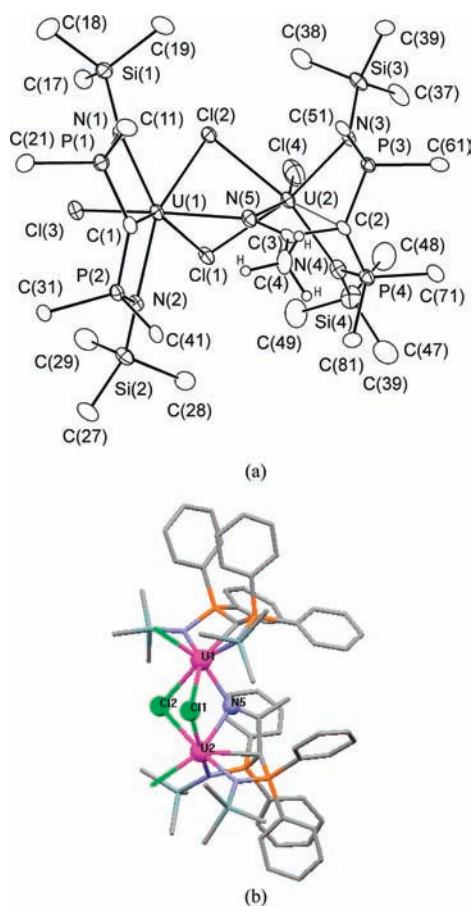


Figure 3. (a) Perspective view of the $[\{(\text{Me}_3\text{SiN}=\text{PPh}_2)_2\text{C}\}\text{ClU}(\mu\text{-Cl})_2\text{UCl}\{\text{NC}(\text{Me})\text{C}(\text{Ph}_2\text{P}=\text{NSiMe}_3)_2\}]$ (**9**) molecule showing the atom labeling scheme. Non-hydrogen atoms are represented by Gaussian ellipsoids at the 20% probability level. Only the ipso carbon atoms attached to phosphorus are shown. Hydrogen atoms attached to C(4) are shown with arbitrarily small thermal parameters and are not numerically designated; all other hydrogen atoms are not shown. (b) View of the trigonal bipyramid formed by the two uranium centers and the three bridging atoms.

to a single metal–carbon bond with the insertion of the nitrile CN unit. As shown in Figure 3b, the three bridging atoms Cl(1), Cl(2), and N(5) define a plane with the two uranium metals sitting above and below the plane. This core adopts a trigonal bipyramidal shape. Uranium(2), which is coordinated by three nitrogen atoms and one carbon atom of the tetradentate ligand, forms a set of three planes jointly sharing the axis defined by U(2) and C(2) atoms, with a dihedral angle of approximately 120° . The uranium-bound terminal chlorides show shorter U–Cl bond distances (2.522(5) Å or 2.660(2) Å) compared to those to the chlorides which bridge the uranium atoms (2.8941(17) Å or 2.9313(18) Å). In addition, the bond angle of P(1)–C(1)–P(2) ($144.4(4)^\circ$) incorporating the U=C double bond in U(1)) is slightly smaller than that in **5** ($149.84(14)^\circ$) and larger than that in **7** ($138.49(17)^\circ$). This angle is larger than the P(3)–C(2)–P(4) ($126.1(4)^\circ$) based on the U–C single bond to U(2).

Theoretical Calculations. The most interesting feature of these Th(IV) and U(IV) PCP methanediide structures is the presence of short metal–carbon bond distances. In order to fully understand the nature of this metal–carbene bond interaction, we have carried out DFT calculations with Gaussian 03^{15,11b}

Table 3. Selected Bond Lengths (Å) and Angles (deg) for Complex **9**

bond lengths (Å)			
U(1)–C(1)	2.337(7)	U(2)–C(2)	2.660(7)
U(1)–N(1)	2.465(6)	U(2)–N(3)	2.456(6)
U(1)–N(2)	2.432(6)	U(2)–N(4)	2.354(7)
U(1)–N(5)	2.412(6)	U(2)–N(5)	2.383(6)
U(1)–Cl(1)	2.9313(18)	U(2)–Cl(1)	2.7717(18)
U(1)–Cl(2)	2.8941(17)	U(2)–Cl(2)	2.782(2)
U(1)–Cl(3)	2.660(2)	U(2)–Cl(4)	2.522(5)
P(1)–C(1)	1.674(7)	P(3)–C(2)	1.729(6)
P(2)–C(1)	1.681(7)	P(4)–C(2)	1.754(7)
P(1)–N(1)	1.635(6)	P(3)–N(3)	1.617(6)
P(2)–N(2)	1.605(6)	P(4)–N(4)	1.615(7)
		C(2)–C(3)	1.570(9)
		N(5)–C(3)	1.268(9)
		C(3)–C(4)	1.490(10)
angles (deg)			
P(1)–C(1)–P(2)	144.4(4)	P(3)–C(2)–P(4)	126.1(4)
U(1)–N(5)–U(2)	108.7(3)	P(3)–C(2)–C(3)	114.7(5)
U(1)–Cl(1)–U(2)	86.14(5)	P(4)–C(2)–C(3)	118.2(4)
U(1)–Cl(2)–U(2)	86.67(5)	C(2)–C(3)–C(4)	118.4(6)
Cl(2)–U(1)–Cl(3)	95.40(6)	N(5)–C(3)–C(2)	116.9(6)
Cl(2)–U(2)–Cl(4)	87.81(11)	N(5)–C(3)–C(4)	124.7(6)

using as models $[\text{Cp}_2\text{Th}\{\text{C}(\text{Me}_2\text{P}=\text{NSiH}_3)_2\}]$ (**4a**), $[\text{Cp}_2\text{U}\{\text{C}(\text{Me}_2\text{P}=\text{NSiH}_3)_2\}]$ (**5a**), $[\text{TpTh}\{\text{C}(\text{Me}_2\text{P}=\text{NSiH}_3)_2\}\text{Cl}]$ (**6a**), and $[\text{TpU}\{\text{C}(\text{Me}_2\text{P}=\text{NSiH}_3)_2\}\text{Cl}]$ (**7a**) to probe the nature of the core structure. We performed closed shell Hartree–Fock calculations on all model systems (**4a–7a**); however, because the two U(IV) compounds (**5a** and **7a**) possess a $5f^2$ electron configuration with two unpaired electrons, we also performed restricted open shell Hartree–Fock calculations (ROHF) on **5a** and **7a** as well. The result was an additional energy stabilization of approximately 25.0 kcal/mol for (**5a** and **7a**) compared to the closed shell results (for details, see the Supporting Information). Overall, bonding pictures are not substantially affected by the open shell configuration, which shows a double bonding interaction between the metal (Th or U) and the carbene centers.

For thorium compound **4a**, the highest occupied molecular orbitals (HOMOs; MO = 110, $E = -0.190$ au) and the HOMO–1 (MO = 109, $E = -0.200$ au) show individual π and σ multiple bond components between the carbene center and the metal thorium center (Figure 4, top). The molecular orbital coefficients indicate that this molecular orbital (HOMO, MO–110) is formed by interaction between the carbene p_z atomic orbital and (mainly) part of the Th 6d orbital, with two electrons of the carbene p_z providing a π lone pair donation to the Th 6d orbital to form a π bond. HOMO–1 (MO–109) is formed between the p_y carbene orbital (which is best described as one σ component of an approximately sp^2 set) and part of the Th 6d. Two electrons of this σ component provided as a σ lone pair donation to the Th 6d orbital to form a σ bond. A natural bond orbital (NBO) analysis of **4a** also reveals the double carbene metal bonds (C–Th) with 5.7% Th and 94.3% carbene (NBO orbitals in Figure 4, bottom; for details, see the Supporting Information). This indicates

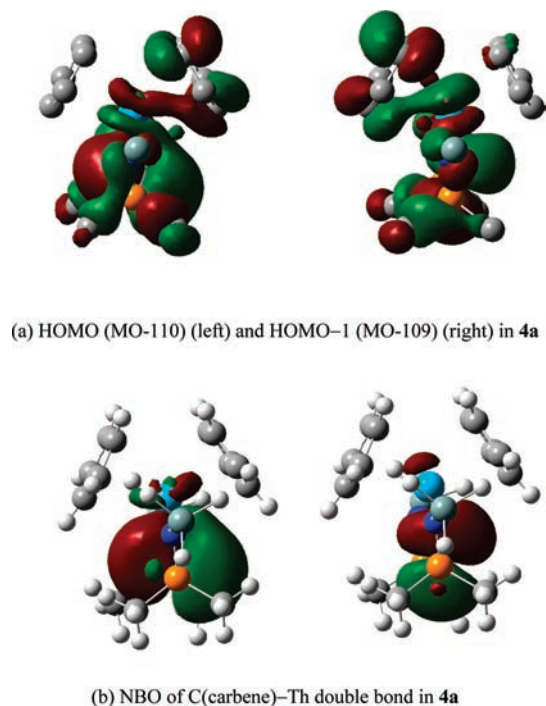


Figure 4. (a) HOMO (MO-110) and HOMO-1 (MO-109) of $[\text{Cp}_2\text{Th}\{\text{C}(\text{Me}_2\text{P}=\text{NSiH}_3)_2\}]$ (**4a**), which represent individual double bonding C=Th components. (b) NBO of C(carbene)-Th double bond in **4a** (π and σ bonds).

the main contribution to the double bond from the carbene center, and it is consistent with dianion carbene character.

For the uranium compound **5a**, the highest occupied molecular orbitals HOMO (MO-112, $E = -0.058$ au) and HOMO-1 (MO-111, $E = -0.062$ au) have almost pure $5f$ atomic orbital (AO) character (with also a small bonding interaction with the carbons of the two Cp ligands), while HOMO-2 (MO-110, $E = -0.193$ au) and HOMO-3 (MO-109, $E = -0.207$ au) are the individual π and σ multiple bond components formed between the diide carbon and the metal (U) orbital components (Figure 5a). The molecular orbital coefficients indicate that in **5a** the formation of the σ bond involves one lobe (which is dominated by the p character: 16% s and 84% p) of the carbene center σ hybrid overlapping with a mix of the $6s^{0.09}$, $6d^{0.22}$, and $5f^{0.68}$ uranium orbitals, dominated by the latter. A second (π) bond is formed by the p_z carbene orbital (which is 100% p) overlapped with a metal $6d^{0.18}5f^{0.88}$ orbital combination. A natural bond orbital (NBO) analysis of **5a** reveals the double carbene metal bond character (C-U) with 12.0% U and 88.0% carbene in **5a** (Figure 5b, for details, see the Supporting Information). Wiberg bond indices are 0.4582 and 0.6619 for C=Th and C=U, respectively, indicating that the C=U bond is stronger than the C=Th bond, which is consistent with the relative C-Th and C-U bond distances in **4** and **5**. When compared to Wiberg bond indices of N-Th (**4**: 0.258) and N-U (**5**: 0.300) bonds, it is clear that the M=C binding in **4** and **5** has an order higher than one. The very wide P(1)-C(1)-P(2) angle suggests that the σ structure about C(1) is not a true sp^2 hybrid.

The DFT calculations reveal that the bond structures of **6a** and **7a** are similar; the HOMO-2 (137, $E = -0.127$ au) and HOMO-1 (138, $E = -0.108$ au) of **6a** and the HOMO-4 (137, $E = -0.231$ au) and HOMO-3 (138, $E = -0.209$ au) of **7a** show that carbene p_x orbitals are used for formation of a

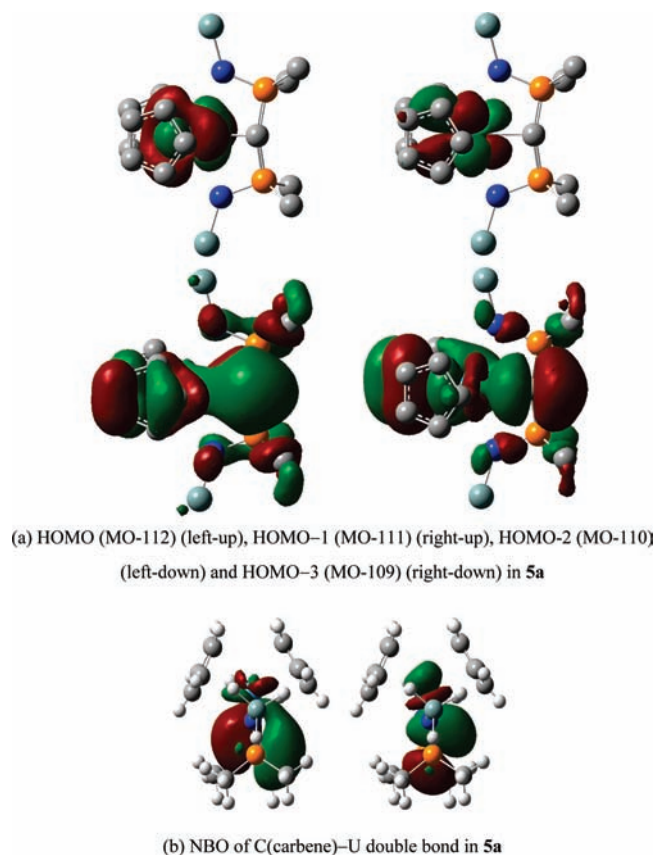
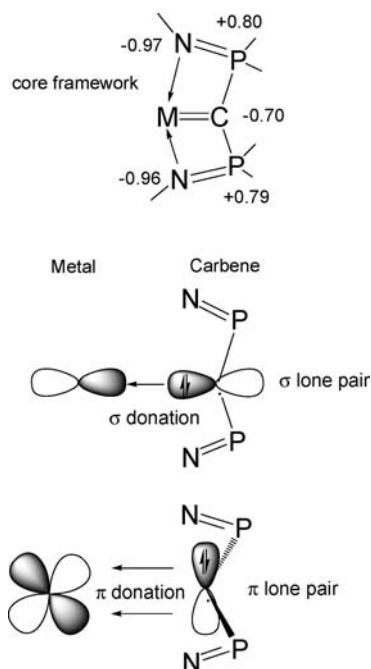


Figure 5. (a) HOMO (MO-112), HOMO-1 (MO-111), HOMO-2 (MO-110), and HOMO-3 (MO-109) of $[\text{Cp}_2\text{U}\{\text{C}(\text{Me}_2\text{P}=\text{NSiH}_3)_2\}]$ (**5a**). HOMO-2 and HOMO-3 represent individual double bonding C=U components. (b) NBO of C(carbene)-U double bond components in **5a** (π and σ bonds).

σ bond and the carbene p_z orbitals are used to form the π bond between the carbene center and the Th and U metal $6d$ and $5f$ orbitals. Overall, the core M=C bond structures of **6a** and **7a** are very similar to those of **4a** and **5a** despite the differences in coordination geometry. A natural bond orbital (NBO) analysis of **6a** and **7a** reveals the carbene metal bonds (C-Th or C-U) with approximately 7.0% Th and 93.0% carbene in **6a** and 12.8% U and 87.2% carbene in **7a** in character (Supporting Information). We suspect that the multiple M (thorium and uranium)-carbon bonds in **4**-**7** are stabilized by balanced, strong coordination to the Cp and Tp ligands and by the chelating imine donation. It is interesting that the core carbene-metal orbitals may appear either as the HOMO and next lowest frontier orbital or, in other cases, somewhat below the frontier levels, which one would think would perturb the potential reactivity. This appears to arise through the subtle interplay between the metal and the other ligand (e.g. Cp or Tp) orbitals and the core pincer (NPCPN) structure. What influence this has on the reactivity of each complex particularly with respect to overall nucleophilicity of the M=C center needs to be further explored.

DFT calculations for related carbene complexes of uranium with the geminal dianion SCS^{2-} carbene were reported recently in the literature.^{8a,16} In principle, our NPCPN carbene has the same central coordination properties as SCS^{2-} , and the ligand systems belong to the same methandiide family, so it is not surprising to see very similar actinide M=C double bond bonding

Scheme 3. Formation of a $M=C$ Double Bond upon Coordination of the Carbene Dianion to an Electron Deficient Metal Center



structures in both complexes. Overall, all results demonstrate that ligand **1** behaves as a dianionic carbene center through the donation of two carbon electron pairs on the dianion (a $\pi(p_z)$ and a $\sigma(p_x)$ N–P–C–P–N framework set (made up of p_y and p_x and s components) to metal-centered vacant orbitals, which results in the formation of an $M=C$ double bond (Scheme 3). We also show the Mulliken charges in Scheme 3, which (although not completely accurate) reflect a zwitterionic delocalization throughout the core structure.

Interestingly, complexes **4** (**5**) and **6** (**7**) show very similar thorium (uranium) to carbon bonding, but **6** and **7** differ from **4** and **5** in that a chloride is also bound to the actinide metal, forcing an increase in coordination to 7 in the **6** and **7** pair. In addition, the Tp ligand imposes smaller steric constraints than Cp, so it will be interesting to see if the Th and U centers in **6** and **7** can be further functionalized.

SUMMARY AND CONCLUSION

Treating uranium or thorium tetrachloride with dilithium-bis(iminophosphorano)methandiide gave U or Th metal carbene complexes which were derivatized for crystallinity. These four complexes (**4**–**7**) represent additional extensions of actinides bound to a dianionic carbene bis(iminophosphorano)methandiide ligand system, which exhibits bonding properties similar to those of the analogous actinide dianionic bis(thiophosphoryl)methandiide. The complexes **4** and **6** are the first examples of Th complexes of this system.

All complexes present short $M-C$ bond distances. The planarity at the carbene center favors the donation of the σ and π structures of the carbon to the actinide (U or Th) center, leading to formation of a “double” bond with marked shortening of the U –carbene distance. Gaussian 03 DFT calculations clearly

indicated electron transfer from the carbon to the metal center. The DFT calculations show that the components of the $M=C$ double bond involve the $5f$ and $6d$ orbitals of the actinide metal and the carbene $2p$ orbitals, as both π bond and σ bond components. The chemical reactivity of the multiple $U=C$ double bond in **3** with either acetonitrile or benzonitrile substrates was established. The nitrile cycloadds to the $M=C$ bond to form a new $C-C$ bond building a new tetradentate chelating ligand with a carbon imine center which subsequently coordinates and binds through this new imine nitrogen with another equivalent of untransformed carbene to form a dimeric, dimetallic complex. The cycloaddition reduces the $M=C$ bond to a $M-C$ bond; thus, the final dimetallic complex contains two U –carbon bond types with the expected difference in bond lengths.

Some contrasting reactivity between the imino NCN^{2-} and thiophosphoryl SCS^{2-} systems was observed, and additional studies of these systems warrant further investigation. Our work on imino coordinated systems continues.

EXPERIMENTAL SECTION

General Methods. All experimental manipulations were performed under rigorously anaerobic conditions using Schlenk techniques or an argon-filled glovebox. Solvents used (special THF, toluene, and ether) were dried over appropriate drying agents and degassed by three freeze–pump–thaw cycles prior to use. The 1H , ^{13}C , and ^{31}P NMR spectra were recorded on a Varian I400 spectrometer operating at 400.13, 100.6, and 161.9 MHz, respectively. The 1H and ^{13}C NMR spectra are referenced internally using the residual proton solvent resonances, which were referenced to $SiMe_4$ ($\delta = 0$). ^{31}P NMR chemical shifts are given relative to an 85% H_3PO_4 external reference. Elemental analyses and IR spectra were carried out at the Analytical and Instrumentation Laboratory, Department of Chemistry, University of Alberta. The organolithium compound $[Li_2L]_2$ (**1**) was prepared according to our published procedures.^{10a,17} $ThCl_4(dme)_2$ and UCl_4 , which had been prepared according to published procedures,¹⁸ were donated by Prof. Josef Takats, Department of Chemistry, University of Alberta. All other chemicals were purchased from either Strem or Aldrich.

Crystal Structure Determination. Suitable crystals of **4**–**9** were mounted on glass fibers by means of mineral oil, and data were collected using graphite-monochromated Mo $K\alpha$ radiation (0.71073 Å) on a Bruker PLATFORM/SMART 1000 CCD diffractometer. The structures were solved by direct methods using SHELXL-86^{19a} and refined using full-matrix least-squares on F^2 (SHELXL-93).^{19b} All of the non-hydrogen atoms in the structure compound were refined with anisotropic displacement parameters. Selected crystal data and structure refinement details for all of the compounds are listed in Table 4.

Synthesis of $[Cp_2Th\{C(Ph_2P=NSiMe_3)_2\}]$ (4**).** To a colorless THF (5 mL) solution of $ThCl_4(DME)_2$ (0.111 g, 0.2 mmol) was added solid $[Li_2C(Ph_2P=NSiMe_3)_2]_2$ (0.115 g, 0.1 mmol) with stirring at room temperature. The reaction mixture was stirred at room temperature for 2 h, providing a brown-orange solution, to which was added solid, brown-red, thallium(I) cyclopentadienide, $TiCp$ (0.108 g, 0.4 mmol). The reaction mixture was kept overnight at room temperature while maintaining vigorous stirring. The white precipitate of $TiCl$ was decanted by centrifugation. The THF solvent was removed under vacuum conditions, and the remaining powder was dissolved in 10 mL of ether. The insoluble solid $LiCl$ was decanted by centrifugation. The resultant red solution was reduced to half of the volume under vacuum conditions and put inside a -20 °C freezer for two days. A red crystalline solid was obtained. The product was filtered and dried under vacuum conditions. Yield: 0.103 g, 56.0%. IR data (Nujol mull): 3057 m, 2949s,

Table 4. Crystal Data and Structure Refinement Details for Complexes 4–9

empirical formula	C ₄₁ H ₄₈ N ₂ - P ₂ Si ₂ Th (4)	C ₄₁ H ₄₈ N ₂ - P ₂ Si ₂ U ₆ (5)	C ₄₀ H ₄₈ BClN ₈ - P ₂ Si ₂ Th (6)	C ₄₀ H ₄₈ BClN ₈ - P ₂ Si ₂ U (7)	C ₁₃ H ₂₁ Cl ₃ O ₂ U (8)	C ₇₆ H ₁₀₇ Cl ₄ N ₅ - P ₄ Si ₄ U ₂ (9)
fw	918.97	924.96	1037.28	1043.27	553.68	1944.77
cryst syst	triclinic	triclinic	orthorhombic	orthorhombic	monoclinic	trigonal
space group	<i>P</i> (No. 2)	<i>P</i> (No. 2)	<i>P</i> 2 ₁ 2 ₁ 2 ₁ (No. 19)	<i>P</i> 2 ₁ 2 ₁ 2 ₁ (No. 19)	<i>P</i> 2 ₁ / <i>c</i> (No. 14)	R3c (No. 161)
unit cell parameters						
<i>a</i> (Å)	10.263(2)	10.2290(6)	10.5465(6)	10.5116 (9)	8.3657 (9)	45.586 (4)
<i>b</i> (Å)	11.750(3)	11.7512(7)	18.4379(11)	18.3976 (15)	13.3438 (14)	
<i>c</i> (Å)	17.920(4)	17.8708(10)	22.7463(13)	22.7622 (19)	15.4265 (16)	21.7302 (14)
α (deg)	74.871(3)	74.6909(7)				
β (deg)	76.889(3)	76.9568(7)			101.9790(10)	
γ (deg)	76.480(3)	76.4559(7)				
volume (Å ³)	1996.3(8)	1983.3(2)		4401.9 (6)	1684.6 (3)	39107 (5)
Z	2	2	4	4	4	18
calculated density (g cm ⁻³)	1.529	1.549	1.558	1.574	1.574	1.486
temperature, K	193.2(1)	193.2(1)	193.2(1)	193.2(1)	193.2(1)	193.2(1)
μ (Mo Kα) (mm ⁻¹)	3.905	4.264	3.597	3.914	10.10	4.015
independent reflns	8988	9044	10088	10014	3845	19943
observed reflns	7926	8507	9498	9521	3633	14958
data/restraints/params	8988/0/433	9044/0/433	10088/0/496	10014/0/496	3845/0/181	19943/0/749
goodness of fit on F ²	1.056	1.078	1.090	1.020	1.154	0.959
final R indices						
[F ₀ ² ≥ 2σ(F ₀ ²)]	R ₁ = 0.0299	R ₁ = 0.0200	R ₁ = 0.0222	R ₁ = 0.0196	R ₁ = 0.0212	R ₁ = 0.0444
wR ₂ [F ₀ ² ≥ 3σ(F ₀ ²)]	wR ₂ = 0.0879	wR ₂ = 0.0503	wR ₂ = 0.0578	wR ₂ = 0.0437	wR ₂ = 0.0538	wR ₂ = 0.106
large difference peak and hole	-0.766 and 2.164 e/Å ³	-0.343 and 1.244 e/Å ³	-0.516 and 1.106 e/Å ³	-0.403 and 1.203 e/Å ³	-1.115 and 1.081 e/Å ³	-0.683 and 3.187 e/Å ³

2894w, 1438s, 1298, 1275s, 1240s, 1159 m, 1114s, 1014 m, 830s, 746s, 694s. ¹H NMR (THF-d₈): δ 7.37 (m, phenyl, 8H), 7.26 (t, phenyl, 4H), 7.15 (t, phenyl, 8H), 6.41 (s, C₅H₅, 10H), -0.02 (s, Si(CH₃)₃, 18H). ¹³C{¹H} NMR (THF-d₈): δ 139.55 (d, phenyl), 131.70 (t, phenyl), 130.34 (s, phenyl), 128.41 (t, phenyl), 117.18 (s, C₅H₅), 4.32 (s, Si(CH₃)₃). ³¹P{¹H} NMR (THF-d₈): δ 4.0 (s). Anal. Calcd for C₄₁H₄₈N₂P₂Si₂Th: C, 53.58; H, 5.26; N, 3.05. Found: C, 53.13; H, 5.33; N, 3.00.

Synthesis of [Cp₂U{C(Ph₂P=NSiMe₃)₂}] (5). A similar procedure to that for 4 was used. Yield: 0.113 g, 61.1%. IR data (Nujol mull): 3058 m, 2953s, 1438s, 1313w, 1241 m, 1124s, 1070 m, 1016 m, 882s, 743s, 691s. ¹H NMR (THF-d₈): δ 14.27 (s, phenyl, 8H), 9.16 (t, phenyl, 8H), 8.31 (t, phenyl, 4H), -14.21 (s, -Si(CH₃)₃, 18H), -14.79 (s, C₅H₅, 10H). ¹³C{¹H} NMR (THF-d₈): δ 142.11 (br. s, phenyl), 133.51 (br. s, phenyl), 131.56 (br. s, phenyl), 130.60 (s, C₅H₅), 128.04 (s, phenyl), 3.40 (s, Si(CH₃)₃). ³¹P{¹H} NMR (THF-d₈): δ 361.62 (br. s). Anal. Calcd for C₄₁H₄₈N₂P₂Si₂U: C, 53.24; H, 5.23; N, 3.03. Found: C, 53.21; H, 5.29; N, 3.03.

Synthesis of [{HB(pyrazolyl)₃}Th{C(Ph₂P=NSiMe₃)₂}] (6). A similar procedure to that for 4 was used, except that 1 equiv of TpK was added in the second step in place of TICp. Yield: 0.125 g, 60.3%. IR data (Nujol mull): 3056 m, 2925 m, 2447s 1590s, 1573s, 1500 m, 1482w, 1436w, 1296 m, 1110s, 1043s, 965s, 926 m, 876 m, 828 m, 747s, 703s, 693 m. ¹H NMR (THF-d₈): δ 7.71 (m, pyrazolyl, 3H), 7.56 (m, pyrazolyl, 3H), 7.32 (m, phenyl, 8H), 7.29 (m, phenyl, 4H), 7.19 (t, phenyl, 8H), 6.00 (t, pyrazolyl, 3H), -0.15 (s, Si(CH₃)₃, 18H). The B–H signal was not observed in ¹H NMR, as it is frequently broad; however, the IR peak at 2447 cm⁻¹ and the crystal structure confirm the presence of B–H. ¹³C{¹H} NMR (THF-d₈): δ 142.51 (s, pyrazolyl), 139.51 (s, phenyl), 137.56 (s, pyrazolyl), 132.11 (s, phenyl), 131.11 (s, phenyl), 128.03 (s, phenyl), 103.63 (s, pyrazolyl), 4.32 (s, Si(CH₃)₃). ³¹P{¹H} NMR (THF-d₈): δ 17.7 (s). Anal. Calcd for C₄₀H₄₈BClN₈P₂Si₂Th: C, 46.31; H, 4.66; N, 10.80. Found: C, 46.16; H, 4.75; N, 10.78.

Synthesis of [{HB(pyrazolyl)₃}U{C(Ph₂P=NSiMe₃)₂}] (7). A similar procedure to that for 4 was used. Yield: 0.110 g, 53%. IR data (Nujol mull): 3056 m, 2949s, 2892 m, 2456s 1501s, 1436s, 1401w, 1386w, 1299s, 1273w, 1240 m, 1216 m, 1116s, 1048s, 975 m, 920 m, 860 m, 829 m, 741s, 724 m, 692 m. ¹H NMR (THF-d₈): δ 15.15 (d, phenyl, 8H), 9.49 (t, phenyl, 8H), 8.96 (t, phenyl, 4H), 5.39 (t, pyrazolyl, 3H), 5.09 (s, -Si(CH₃)₃, 18H), 4.22 (br. t, pyrazolyl, 3H), -2.00 (very br. pyrazolyl, 3H). As above, the B–H signal was not observed in ¹H NMR, and in this case the paramagnetic broadening will likely obscure this signal. However, the IR peak at 2456 cm⁻¹ and the crystal structure confirm the presence of B–H. ¹³C{¹H} NMR (THF-d₈): δ 149.96 (d, pyrazolyl), 138.52 (br. s, phenyl), 135.79 (s, pyrazolyl), 133.65 (s, phenyl), 130.12 (s, phenyl), 123.56 (s, phenyl), 102.65 (s, pyrazolyl), -1.38 (s, Si(CH₃)₃). ³¹P{¹H} NMR (THF-d₈): δ -382.0 (br. s). Anal. Calcd for C₄₀H₄₈BClN₈P₂Si₂U (THF): C, 47.38; H, 5.06; N, 10.05. Found: C, 47.10; H, 4.95; N, 10.05.

Synthesis of [CpUCl₃(THF)₂] (8). To a green THF (5 mL) solution of UCl₄ (0.076 g, 0.2 mmol) was added solid, brown-red thallium(I) cyclopentadienide TICp (0.074 g, 0.2 mmol) with stirring at room temperature. The reaction mixture was kept overnight at room temperature with vigorous stirring. The white precipitate of TICl was decanted by centrifugation. The THF solvent was evaporated slowly for a few days, and deep green solid brick crystals were collected. Yield: 0.085 g, 77%. The IR, element analysis, and ¹H NMR were carried out in the previous works.^{13b}

Computational Details. DFT calculations of core structures of 4a, 5a, 6a, and 7a were performed with Gaussian 03¹⁵ using the closed shell Hartree–Fock and the restricted open shell Hartree–Fock (ROHF) with B3PW91 functional for Th and U compounds, respectively; the SDD basis set of MWB60 on Th and U; the 6-311G basis set on P and N; and 6-31G on Si, C, and H. The phenyl ring on phosphorus was replaced with methyl, and methyl on silicon was replaced with H. The SDD basis is constructed with a quasirelativistic effective core potential that allows the incorporation of scalar relativistic effects in nonrelativistic calculations.^{11b}

■ ASSOCIATED CONTENT

S Supporting Information. Atomic positions and displacement parameters, anisotropic displacement parameters, bond lengths and bond angles in CIF format. Table of crystal structural data and computed input files for all the calculated model compounds (**4a**, **5a**, **6a**, and **7a**). This material is available free of charge via the Internet at <http://pubs.acs.org>.

■ AUTHOR INFORMATION

Corresponding Author

*Telephone 780-492-5310. Fax 780-492-8231. E-mail: ron.cavell@ualberta.ca.

■ ACKNOWLEDGMENT

We thank the Natural Sciences and Engineering Research Council of Canada and the University of Alberta for financial support. The authors also thank Prof. Josef Takats for kindly donating the Th and U precursors and the University of Alberta for supporting the X-ray Crystallography, NMR, and Analytical and Instrumentation laboratories at the Department of Chemistry.

■ REFERENCES

- (1) (a) Arduengo, A. J. *Acc. Chem. Res.* **1999**, *32*, 913–926. (b) Herrmann, W. A. *Angew. Chem., Int. Ed.* **2002**, *41*, 1290–1309. (c) Howard, T. R.; Lee, J. B.; Grubbs, R. H. *J. Am. Chem. Soc.* **1980**, *102*, 6876–6878. (d) Bielawski, C. W.; Grubbs, R. H. *Angew. Chem., Int. Ed.* **2000**, *39*, 2903–2906.
- (2) (a) Collman, J. P.; Hegedus, L. S. *Principles and Applications of Organotransition Metal Chemistry*; University Science Books: Mill Valley, CA, 1980; Chapters 3.4 and 11 or 1987; pp 475. (b) Davidson, P. J.; Lappert, M. F.; Pearce, R. *Chem. Rev.* **1976**, *76*, 219–268. (c) Doyle, M. P.; Forbes, D. C. *Chem. Rev.* **1998**, *98*, 911–935. (d) Vyboishchikov, S. F.; Frenking, G. *Chem.—Eur. J.* **1998**, *4*, 1428–1438. (e) Brothers, P. J.; Roper, W. R. *Chem. Rev.* **1988**, *88*, 1293–1326. (f) Erker, G. *Angew. Chem., Int. Ed. Engl.* **1989**, *28*, 397–412. (g) Feldman, J.; Schrock, R. R. *Prog. Inorg. Chem.* **1991**, *39*, 1–74. (h) Wulff, W. D. *Organometallics* **1998**, *17*, 3116–3134. (i) Brookhart, M.; Studabaker, W. B. *Chem. Rev.* **1987**, *87*, 411–432.
- (3) (a) Gottfriedsen, J.; Edelmann, F. T. *Coord. Chem. Rev.* **2007**, *251*, 142–202 and refs therein. (b) Fagan, P. J.; Manriquez, J. M.; Maatta, E. A.; Seyam, A. M.; Marks, T. J. *J. Am. Chem. Soc.* **1981**, *103*, 6650–6667. (c) Arney, D. S. J.; Burns, C. J.; Smith, D. C. *J. Am. Chem. Soc.* **1992**, *114*, 10068–10069. (d) Hayton, T. W.; Boncella, J. M.; Scott, B. L.; Palmer, P. D.; Batista, E. R.; Hay, P. J. *Science* **2005**, *310*, 1941–1943. (e) Hayton, T. W.; Boncella, J. M.; Scott, B. L.; Batista, E. R.; Hay, P. J. *J. Am. Chem. Soc.* **2006**, *128*, 10549–10559. (f) Cramer, R. E.; Maynard, R. B.; Paw, J. C.; Gilje, J. W. *J. Am. Chem. Soc.* **1981**, *103*, 3589–3590. (g) Cramer, R. E.; Maynard, R. B.; Paw, J. C.; Gilje, J. W. *Organometallics* **1983**, *2*, 1336–1340. (h) Warner, B. P.; Scott, B. L.; Burns, C. J. *Angew. Chem., Int. Ed.* **1998**, *37*, 959–960. (i) Stevens, R. C.; Bau, R.; Cramer, R. E.; Afzal, D.; Gilje, J. W.; Koetzle, T. F. *Organometallics* **1990**, *9*, 694–697. (j) Korobkov, I.; Gorelsky, S.; Gambarotta, S. *J. Am. Chem. Soc.* **2009**, *131*, 10406–10420. (k) Fortier, S.; Melot, B. C.; Wu, G.; Hayton, T. W. *J. Am. Chem. Soc.* **2009**, *131*, 15512–15521. (l) Evans, W. J.; Siladka, N. A.; Ziller, J. W. *Chem.—Eur. J.* **2010**, *16*, 796–800.
- (4) (a) Oldham, W. J., Jr.; Oldham, S. M.; Scott, B. L.; Abney, K. D.; Smith, W. H.; Costa, D. A. *Chem. Commun.* **2001**, 1348–1349. (b) Arnold, P. L.; Blake, A. J.; Wilson, C. *Chem.—Eur. J.* **2005**, *11*, 6095–6099. (c) Mehdioui, T.; Berthet, J. C.; Thuery, P.; Ephritikhine, M. *Chem. Commun.* **2005**, 2860–2862.
- (5) (a) Arnold, P. L.; Liddle, S. T. *Chem Commun.* **2006**, 3959–3971. (b) Giesbrecht, G. R.; Gordon, J. C. *Dalton Trans.* **2004**, 2387–2393.
- (6) (a) Andrews, L.; Cho, H. G. *Organometallics* **2006**, *25*, 4040–4053. (b) Lyon, J. T.; Andrews, L.; Hu, H. S.; Li, J. *Inorg. Chem.* **2008**, *47*, 1435–1442.
- (7) (a) Villiers, C.; Ephritikhine, M. *Chem.—Eur. J.* **2001**, *7* (14), 3043–3051. (b) Villiers, C.; Vandais, A.; Ephritikhine, M. *J. Organomet. Chem.* **2001**, *617–618*, 744–747.
- (8) (a) Cantat, T.; Arliguie, T.; Noel, A.; Thuery, P.; Ephritikhine, M.; Le Floch, P.; Mézailles, N. *J. Am. Chem. Soc.* **2009**, *131*, 963–972. (b) Tourneux, J.-C.; Berthet, J.-C.; Thuery, P.; Mézailles, N.; Floch, P. L.; Ephritikhine, M. *Dalton Trans.* **2010**, *39*, 2494–2496. (c) Cooper, O. J.; McMaster, J.; Lewis, W.; Blake, A. J.; Liddle, S. T. *Dalton Trans.* **2010**, *39*, 5074–5076.
- (9) (a) Cavell, R. G.; Kamalesh Babu, R. P.; Kasani, A.; McDonald, R. *J. Am. Chem. Soc.* **1999**, *121*, 5805–5806. (b) Kamalesh Babu, R. P.; McDonald, R.; Decker, S. A.; Klobukowski, M.; Cavell, R. G. *Organometallics* **1999**, *18*, 4226–4229. (c) Kasani, A.; McDonald, R.; Cavell, R. G. *Organometallics* **1999**, *18*, 3775–3777. (d) Aparna, K.; Ferguson, M.; McDonald, R.; Cavell, R. G. *Organometallics* **1999**, *18*, 4241–4243. (e) Kasani, A.; McDonald, R.; Cavell, R. G. *J. Chem. Soc., Chem. Commun.* **1999**, 1993–1994. (f) Babu, R. P. K.; McDonald, R.; Decker, S. A.; Klobukowski, M.; Cavell, R. G. *Organometallics* **1999**, *18*, 4226–4229. (g) Aparna, K.; Ferguson, M.; Cavell, R. G. *J. Am. Chem. Soc.* **2000**, *122*, 726–727. (h) Babu, R. P. K.; McDonald, R.; Cavell, R. G. *Organometallics* **2000**, *19*, 3462–3465. (i) Babu, R. P. K.; McDonald, R.; Cavell, R. G. *Chem. Commun.* **2000**, 481–482. (j) Jones, N. D.; Lin, G.-Y.; Gossage, R. A.; McDonald, R.; Cavell, R. G. *Organometallics* **2003**, *22*, 2832–2841. (k) Fang, M.; Jones, N. D.; Lukowski, R.; Tjathas, J.; Ferguson, M. J.; Cavell, R. G. *Angew. Chem., Int. Ed.* **2006**, *45*, 3097–3101. (l) Cavell, R. G.; Babu, R. P. K.; Aparna, K. *J. Organomet. Chem.* **2001**, *617*, 158–169. (m) Jones, N. D.; Cavell, R. G. *J. Organomet. Chem.* **2005**, *690*, 5485–5496. (n) Cavell, R. G. *The Chemistry of Pincer Compounds*; Morales-Morales, D., Jensen, C. M., Eds.; Elsevier: Amsterdam; Chapter 14, pp 311–346 and refs therein. (o) Ma, G.-B.; McDonald, R.; Cavell, R. G. *Organometallics* **2010**, *29*, 52–60. (p) Ma, G.-B.; Ferguson, M. J.; Cavell, R. G. *Chem. Commun.* **2010**, 5370–5372. (q) Ma, G.; Ferguson, M. J.; McDonald, R.; Cavell, R. G. *Organometallics* **2010**, *29*, 4251–4264. (r) Woolees, A. J.; Cooper, O. J.; McMaster, J.; Lewis, W.; Blake, A.; Liddle, S. T. *Organometallics* **2010**, *29*, 2315–2321.
- (10) (a) Kasani, A.; Kamalesh, B. R. P.; McDonald, R.; Cavell, R. G. *Angew. Chem., Int. Ed. Engl.* **1999**, *38*, 1483–1484. (b) Ong, C. M.; Stephan, D. W. *J. Am. Chem. Soc.* **1999**, *121*, 2939–2940.
- (11) (a) Pool, J. A.; Scott, B. L.; Kiplinger, J. L. *J. Am. Chem. Soc.* **2005**, *127*, 1338–1339. (b) Carlson, C. N.; Hanusa, T. P.; Brennessel, W. W. *J. Am. Chem. Soc.* **2004**, *126*, 10550–10551.
- (12) (a) Avis, M. W.; Elsevier, C. J.; Veldman, N.; Kooijman, H.; Spek, A. L. *Inorg. Chem.* **1996**, *35*, 1518–1528. (b) Crystal structure of CH₂{Cy₂P=N(SiMe₃)₂}; Kamalesh, B. R. P.; Cavell, R. G.; McDonald, R. Report RGC 9802, University of Alberta Structure Determination Laboratory: Alberta, Canada.
- (13) (a) Doretti, L.; Zanella, P.; Faraglia, G.; Faleschini, S. *J. Organomet. Chem.* **1972**, *43*, 339–341. (b) Bagnall, K. W.; Edwards, J. J. *Organomet. Chem.* **1974**, *80*, C14–C16. (c) Ernst, R. D.; Kennelly, W. J.; Day, C. S.; Day, V. W.; Marks, T. J. *J. Am. Chem. Soc.* **1979**, *101*, 2656–2664.
- (14) (a) Cramer, R. E.; Maynard, R. B.; Paw, J. C.; Gilje, J. W. *Organometallics* **1982**, *1*, 869–871. (b) Cramer, R. E.; Panchanatheswaran, K.; Gilje, J. W. *J. Am. Chem. Soc.* **1984**, *106*, 1853–1854.
- (15) Frisch, M. J. *Gaussian 03*, Revision C.02; Gaussian, Inc.: Wallingford, CT, 2004. Full citation given in the Supporting Information.
- (16) Cantat, T.; Mézailles, N.; Auffrant, A.; Le Floch, P. *Dalton Trans.* **2008**, 1957–1972.
- (17) Klobukowski, M.; Decker, S. A.; Lovallo, C. C.; Cavell, R. G. *THEOCHEM* **2001**, *536*, 189–194.
- (18) (a) Herrmann, J. A.; Suttle, J. F. *Inorg. Synth.* **1957**, *5*, 143–145. (b) Cantat, T.; Scott, B. L.; Kiplinger, J. L. *Chem. Commun.* **2010**, 919–921.
- (19) (a) Sheldrick, G. M. *Acta Crystallogr.* **1990**, *A46*, 467–473. (b) Sheldrick, G. M. *SHELXL-93*; University of Göttingen: Göttingen, Germany, 1993.